

# 1971 ANNUAL REPORT ON THE INVESTIGATION OF CRITICAL BURNING OF FUEL DROPLETS

by

C. B. Allison, G. S. Canada, and G. M. Faeth

Mechanical Engineering Department  
The Pennsylvania State University  
University Park, Pennsylvania

prepared for

NATIONAL AERONAUTICS AND SPACE ADMINISTRATION  
CONTRACT NGR-39-009-077

Technical Management  
NASA Lewis Research Center  
Cleveland, Ohio  
Dr. R. J. Priem

(NASA-CR-120879) INVESTIGATION OF CRITICAL  
BURNING OF FUEL DROPLETS Annual Report,  
1971 C.B. Allison, et al (Pennsylvania  
State Univ.) Jan. 1972 34 p CSCI 211

G3/33

Unclas  
25452

N72-23945

## NOTICE

This work was prepared as an account of Government sponsored work. Neither the United States, nor the National Aeronautics and Space Administration (NASA), nor any person acting on behalf of NASA:

- A.) Makes any warranty or representation, expressed or implied, with respect to the accuracy, completeness, or usefulness of the information contained in this report, or that the use of any information apparatus, method, or process disclosed in this report may not infringe privately owned rights; or
- B.) Assumes any liabilities with respect to the use of, or for damages resulting from the use of any information, apparatus, method or process disclosed in this report.

As used above, "person acting on behalf of NASA" includes any employee or contractor of NASA, or employee of such contractor, to the extent that such employee or contractor of NASA, or employee of such contractor prepares, disseminates, or provides access to any information pursuant to his employment or contract with NASA, or his employment with such contractor.

1. Report No. NASA CR-120879		2. Government Accession No.		3. Recipient's Catalog No.	
4. Title and Subtitle 1971 ANNUAL REPORT ON THE INVESTIGATION OF CRITICAL BURNING OF FUEL DROPLETS				5. Report Date January, 1972	
				6. Performing Organization Code	
7. Author(s) C. B. Allison, G. S. Canada, and G. M. Faeth				8. Performing Organization Report No.	
				10. Work Unit No.	
9. Performing Organization Name and Address Mechanical Engineering Department The Pennsylvania State University University Park, Pennsylvania 16802				11. Contract or Grant No. NGR 39-009-077	
				13. Type of Report and Period Covered Contract Report	
12. Sponsoring Agency Name and Address National Aeronautics and Space Administration Washington, D. C. 20546				14. Sponsoring Agency Code	
15. Supplementary Notes Project Manager, Richard J. Priem, Chemical Propulsion Division; NASA Lewis Research Center, Cleveland Ohio					
16. Abstract Measurements were made on the burning rate of liquid hydrazine, MMH, and UDMH in a combustion gas environment. The experimental range of these tests involved gas temperatures of 1660-2530°K, oxygen concentrations of 0-42% by mass and droplet diameters (employing both droplets and porous spheres) of 0.11-1.91 cm. at atmospheric pressure. A simplified hybrid combustion theory was developed which was found to correlate the present results as well as the experimental measurements of other investigators. Measurements were also made of the monopropellant strand burning rates and liquid surface temperatures of a number of nitrate ester fuels and hydrazine at elevated pressures. The temperature measurements for the nitrate esters were found to be in good agreement with a theoretical model which allowed for gas solubility in the liquid phase at high pressures. Experimental results were also obtained on the burning rates and liquid surface temperatures of a number of paraffin and alcohol fuels burning in air at pressures up to 72 atm. For these tests, the fuels were burned from porous spheres in a natural convection environment. Analysis of these results as well as tests to extend the range of this data is currently in progress. Initial findings on a pressurized flat flame burner are also described as well as the design of an oscillatory combustion apparatus to test the response of burning liquid fuels.					
17. Key Words (Suggested by Author(s)) Liquid fuel combustion High pressure combustion Hydrazine fuel combustion			18. Distribution Statement Unclassified - Unlimited		
19. Security Classif. (of this report) Unclassified		20. Security Classif. (of this page) Unclassified		21. No. of Pages	22. Price* \$3.75

## Table of Contents

ABSTRACT

SUMMARY

I. INTRODUCTION

II. ATMOSPHERIC PRESSURE FLAT FLAME STUDY

Introduction  
Experimental Apparatus  
Theoretical Analysis  
Results  
Summary and Conclusions

III. LIQUID STRAND COMBUSTION

Introduction  
Experimental Apparatus  
Theoretical Analysis  
Results  
Summary and Conclusions

IV. OSCILLATORY COMBUSTION

Introduction  
Experimental Apparatus

V. HIGH PRESSURE DROPLET COMBUSTION

Introduction  
Experimental Apparatus  
Theoretical Analysis  
Results  
Summary and Conclusions

VI. HIGH PRESSURE FLAT FLAME STUDY

Introduction  
Experimental Apparatus

REFERENCES

FIGURES

DISTRIBUTION

1971 ANNUAL REPORT ON THE INVESTIGATION OF  
CRITICAL PRESSURE BURNING OF FUEL DROPLETS

SUMMARY

This report discusses activities under NASA Contract NGR 39-009-077 for the period January 1, 1971 through December 31, 1971. The work was divided into five phases, the results under each phase may be summarized as follows:

1. Atmospheric Pressure Flat Flame Study. The combustion characteristics of hydrazine, MMH, and UDMH were investigated at atmospheric pressure for both decomposition and oxidation (hybrid combustion) conditions. In order to simulate the high temperature environment of combustion chambers, droplet burning was observed in the combustion products of a flat flame burner. Gas temperatures of 1660-2530°K and oxygen mass fractions of 0.0-0.42 were employed at the droplet position. Both the supported droplet and porous sphere techniques were used to obtain droplet diameters in the range 0.11-1.91 cm. The experimental mass burning rates increased with increasing droplet diameter, ambient temperature, and ambient oxygen concentration. The influence of ambient conditions decreased as droplet diameter increased, particularly for hydrazine. A theoretical hybrid combustion model was developed to aid in correlating the data. This simplified model postulated an infinitely thin decomposition flame surrounded by an infinitely thin oxidation flame. The model was found to correlate the present data as well as other data on hydrazine combustion in the literature over a wide range of experimental conditions. The average error between the correlation and the measurements for all three fuels was less than 20%.
2. Liquid Strand Combustion. These experiments considered the burning of liquid monopropellant strands. Major emphasis was placed on obtaining liquid phase temperature distributions at elevated pressures, although burning rates were also measured. Testing (at pressures up to 82 atm.) and analysis was completed for three nitrate ester fuels. Work is currently in progress for hydrazine (MMH and UDMH did not sustain combustion in this apparatus). The measured strand burning rate of hydrazine increased linearly with pressure in the range 1-20 atm. Since the pressure levels and burning rates for hydrazine are lower than those of the nitrate esters, the apparatus must be modified before accurate liquid temperature measurements can be obtained. These modifications are currently in progress.
3. Oscillatory Combustion. An experimental apparatus is being designed and built to measure the response of a burning liquid monopropellant strand to pressure oscillations. The objective of this study is to measure the response as a function of mean pressure and the amplitude and frequency of the pressure oscillation. The oscillatory pressures will be provided by a rotary valve system. The assembly of this apparatus is currently in progress.

4. High Pressure Droplet Combustion. These experiments considered the combustion of alcohol and paraffin fuels from porous spheres in a high pressure cold gas environment. Measurements are made of both the steady burning rate and the liquid temperature. Testing to date has reached pressures as high as 72 atm and work in progress will extend this range to 100 atm. The burning rate was found to increase with pressure in manner largely attributable to increasing natural convection. The experimental results are also being analyzed theoretically. Several theoretical models are being compared involving low and high pressure treatments of phase equilibria at the droplet surface as well as a number of approaches to gas phase property variations.
  
5. High Pressure Flat Flame Study. A premixed flat flame burner was designed and tested for use in simulating a combustion gas environment for droplet burning rate tests at elevated pressures. This burner was found to be unsatisfactory due to the difficulty in preventing flash-back in the premixed gases at elevated pressures. In order to avoid this difficulty, a diffusion flame burner is currently under development. Droplet burning rate tests with this apparatus will begin following the completion of the cold gas tests described above.

## I. Introduction

The objective of this investigation is to study the combustion and evaporation of liquid fuels at high pressures. Particular emphasis is placed on conditions where the liquid surface approaches the thermodynamic critical point during combustion. This report gives a summary of progress on the investigation for the period January 1, 1971 to December 31, 1971.

Work during this report period was divided into five phases: (1) Atmospheric Pressure Flat Flame Study, where measurements and analysis were made of the droplet burning rates of hydrazine, MMH and UDMH in a combustion gas environment. (2) Liquid Strand Combustion, which considers the analysis of high pressure effects on the equilibrium surface state of a burning liquid monopropellant column. (3) Oscillatory Combustion, which is an investigation of the response of a burning liquid monopropellant to pressure oscillations. (4) High Pressure Droplet Combustion, which involves measurement and analysis of porous sphere burning rates of liquids in a natural convection environment. (5) High Pressure Flat Flame Study, which considers the steady burning of liquids from porous spheres in a high pressure combustion gas environment; as well as environmental problems in high pressure combustion.

In the following sections, the work in each phase is summarized for the report period. Wherever possible, the details of the work are presented by reference to past publications and only material not previously reported is given extended coverage. References 1, 2, 10, 23-25 comprise other reports and papers, resulting from work done on this project, which have appeared during the period of this report.

## II. Atmospheric Pressure Flat Flame Study

### Introduction:

The purpose of this portion of the investigation was to study the combustion characteristics of the hydrazine fuels at atmospheric pressure and high temperature. Since hydrazine and its derivatives are capable of exothermic decomposition, they may be used as monopropellants as well as the fuel component of a bipropellant system. For monopropellant droplet combustion of these fuels, exothermic decomposition of the fuel can occur in the gas phase near the liquid surface under conditions of high relative reactivity (e.g. high ambient temperature and pressure or large droplet diameter). When these propellants are used as a fuel in a bipropellant system, the decomposition region near the liquid surface is surrounded by an oxidation zone. The presence of both decomposition and oxidation zones is often called the two-flame phenomenon of bipropellant (hybrid) combustion of monopropellants.

The fuels specifically tested included hydrazine, monomethylhydrazine (MMH), unsymmetrical dimethylhydrazine (UDMH) and Aerozine 50 (A-50). The

effects of ambient oxygen concentration, ambient temperature, and drop diameter on the burning rate of these fuels were studied using a flat flame burner apparatus. In addition, a hybrid combustion theoretical model was developed to aid in correlating the data.

The finds of this portion of the investigation are reported in detail in Refs. 1-2. These results are briefly summarized in the following, with emphasis on work completed during this report period.

#### Experimental Apparatus:

In order to simulate the high temperature environment found in rocket engine combustion chambers, the experimental work was conducted using a flat flame burner apparatus. This apparatus has been described in detail in Ref. 2. Briefly, the burner consists of a porous bronze disk 5 cm in diameter cooled at its rim and lower surface by contact with a water cooled copper block. The burner was mounted on rails so that it could be rapidly moved to the test position. By operating the burner with mixtures of carbon monoxide, oxygen, nitrogen, and hydrogen, oxygen mass fractions of 0-0.42 and temperatures of 1660-2530°K were obtained at the drop location.

The temperature and composition of the gas leaving the burner were determined from thermochemical calculations allowing for all relevant dissociation reactions and heat loss to the burner. The thermochemical properties required for these calculations were taken from the JANNAF Tables (3). The gas velocity at the droplet location was calculated from the measured mass flux into the burner and the computed properties of the burned gas. A complete tabulation of the computed properties of the burner gas for all test conditions can be found in Ref. 2.

In order to provide a wide range of droplet diameters, droplet burning rates were measured using both the suspended droplet and porous sphere techniques. For the suspended droplet tests, small drops (about 1200 $\mu$  in diameter) of liquid fuel were mounted on a 100 $\mu$  quartz fiber. The time variation of the drop diameter, recorded photographically, yielded the burning rate. For the porous sphere tests, fuel was fed internally to a porous sphere and forced radially outward with a calibrated syringe pump. The fuel feed rate for the steady burning condition (where the sphere was completely wet without dripping) yielded the burning rate directly. Sphere sizes tested were 0.63, 0.95, 1.27, 1.59, and 1.91 cm in diameter.

#### Theoretical Analysis:

The details of the hybrid combustion model are presented in Ref. 2. As illustrated in Fig. 1, the model consists of a spherical droplet surrounded by a decomposition flame of the fuel gas which, in turn, is surrounded by an oxidation flame of the fuel decomposition products.

The stagnant film approximation was used to estimate the effect of forced convection around the droplet. With this approximation the gas phase is taken to be spherically symmetric between the droplet and the

edge of the stagnant layer,  $r_{\infty}$ . The outer radius,  $r_{\infty}$ , was specified from the flow condition at the droplet position.

Using an approach suggested by Spalding and Jain (4), the monopropellant flame was assumed to be infinitely thin and located at the radial position where the unreacted gas flows into the flame surface at the laminar burning velocity of the mixture. A generalized Arrhenius expression was used for the laminar burning velocity,

$$\dot{m} = 4\pi r_I^2 A \exp\left(\frac{-E}{2RT_I}\right)$$

where  $\dot{m}$  is the total mass burning rate,  $r_I$  is the flame radius,  $T_I$  the flame temperature and  $R$  the universal gas constant. The parameter,  $A$ , represents the pre-exponential factor which also carries any pressure dependence of the laminar flame expression;  $E$  is the activation energy. Both  $A$  and  $E$  were assumed to be constant for each fuel at a given total pressure. The values of  $A$  and  $E$  were determined by the best fit of the theory to the present experimental data.

The bipropellant flame was also assumed to be infinitely thin. Its position was determined by the diffusional requirement that fuel decomposition products and oxidizer combine in stoichiometric proportion at the bipropellant flame surface.

#### Results:

The bulk of the data was taken with the ambient gas completely dry. However, some testing was done to determine the influence of water vapor in the ambient gas. It was found that water vapor mole fractions as large as 0.14 had no effect on the experimental burning rates at a given temperature, ambient oxygen concentration, and drop diameter.

Both suspended droplet and porous sphere tests were conducted with A-50. However, a steady burning condition could not be achieved for any test condition with this fuel. For the suspended droplet tests, the liquid A-50 formed bubbles and shattered before sufficient time had elapsed to obtain a diameter history of the droplet. For porous sphere burning, the liquid burst from the surface of the sphere in the form of small droplets; a stable burning condition could not be obtained even for combustion in air at room temperature.

For all three fuels tested, hydrazine, MMH, and UDMH, the burning rate increased with increasing ambient temperature, ambient oxygen concentration, and drop diameter. However, as drop diameter increased, the effect of ambient conditions (temperature, oxygen concentration, and convection) decreased. In addition as drop diameter increased, the experimental mass burning rates deviated from the straight bipropellant solution which neglects the presence of an inner decomposition flame.

Theoretical results for the hybrid model (assuming three different values of the activation energy in Eq. 1) and a bipropellant model are compared with the data for hydrazine in Fig. 2. The bipropellant results

are shown as bands rather than a single curve in order to illustrate the effect of property uncertainties on the results. The computed burning rates were found to be most sensitive to a change in the thermal conductivity of Region A in Figure 1,  $\lambda_{A2}$ , and the limits shown result from a + 20% variation of this parameter. Single curves are shown for the hybrid model since property uncertainties are absorbed in the uncertainty of the value of A which best fits the data (for a given E).

The bipropellant model deviates considerably from the data for the larger drop sizes, indicating the onset of monopropellant effects. The hybrid model can be fitted reasonably well to the data, with the best results being obtained for a temperature independent laminar flame velocity expression (E=0).

A similar plot for hydrazine at a decomposition condition is shown in Fig. 3. In this case, the bipropellant model reduces to a simple evaporation model and the hybrid model reduces to a pure monopropellant combustion model. The evaporation model underpredicts the burning rate by almost an order of magnitude for the largest sphere sizes, while the monopropellant model for E=0 yields the best fit of the data.

Similar trends were noted for MMH and UDMH although the distinction between the hybrid and bipropellant models was less pronounced. The hybrid model with E=0 yielded the best fit of the data for MMH and UDMH particularly for the larger sphere sizes (2).

A direct comparison was made between predicted mass burning rates using the hybrid model and experimental mass burning rates. This comparison for hydrazine is shown in Fig. 4. Also plotted on Fig. 4 are experimental values of hydrazine burning rates available in the literature.

The bulk of the data in Fig. 4 was obtained at atmospheric pressure (5,6,7). The only exception to this was the results of Kosvic and Breen (8) at 7.8 atm. In order to make a prediction for this elevated pressure, the pre-exponential factor, A, was assumed to be proportional to pressure. This corresponds to an overall reaction order of two as reported by Antoine (9) for hydrazine.

The average percent error between predicted and measured hydrazine burning rates in Fig. 4 was 18.8%. Similar comparisons for MMH and UDMH yielded average errors of 17.1 and 18.7%, respectively (2). The overall range of this data comprised droplet diameters of 0.038-1.91 cm, ambient temperatures of 300-2530°K, and ambient oxygen concentrations of 0-100%. The comparison was largely made for data taken at atmospheric pressure, although, as noted above, hydrazine burning rates at 7.8 atm could be correlated by employing the known pressure dependence of the reaction.

#### Summary and Conclusions:

The results indicate that hydrazine, MMH, and UDMH show increasing burning rates with increasing diameter, ambient oxygen concentration and ambient temperature. As monopropellant effects become more important, the burning rate of these fuels is less sensitive to ambient conditions.

Of the three fuels, hydrazine most clearly exhibited combustion effects; MMH and UDMH only showed this behavior at the largest sphere sizes tested.

The hybrid combustion model appears to provide a satisfactory method of correlating the existing experimental data. However, one must use caution in extrapolating outside the range of existing data due to the approximate nature of the analysis. In particular, data on the high pressure combustion of these fuels is extremely limited. Additional experimental data is required before an adequate test of the hybrid model can be made at elevated pressures.

### III. Liquid Strand Combustion

#### Introduction:

The purpose of this portion of the investigation is to study the temperature distribution and dissolved gas concentrations in an evaporating column of liquid fuel. The experimental technique employed the burning of liquid strands of monopropellant fuels since the flow is one dimensional and steady with this system. In addition, the technique is readily adapted for high pressure testing where gas solubility effects become important.

Earlier work employed the nitrate ester fuels and the bulk of these results are reported in Ref. 10. During the present report period, effort was concentrated on the hydrazine fuels although some testing and analysis was also done for the nitrate esters.

#### Experimental Apparatus:

A sketch of the strand burner apparatus employed in this portion of the study is given in Fig. 5. With this technique, liquid fuel is placed in a glass tube contained in a windowed pressure vessel. The vessel is pressurized with nitrogen to the desired test pressure. Following ignition with a heater coil, the fuel burns down the tube. As the liquid propagates past the window in the chamber, the rate of regression of the liquid column as well as the position of the thermocouple in the liquid phase is determined from motion picture shadowgraphs. In addition, the temperature registered by the thermocouple is recorded on an oscillograph with flat frequency response to 2000 Hz.

The pressure vessel has an inside diameter of 6.4 cm with an inside length of 28 cm. The windows of the vessel have a 2.5 cm viewing space. The liquid column was back lighted with a mercury arc lamp. Shadowgraphs were taken with a high speed motion picture camera operating at about 100 frames per second. The film and temperature records were synchronized by a switch closure which deflected a galvanometer on the temperature record and started a light streak on the film. A 100 Hz timing signal was placed on both the film and oscillograph records.

The thermocouples used to record the liquid temperature were constructed with 0.0003 inch O.D. platinum - platinum 10% rhodium butt welded wire. The procedure used to construct the thermocouples is described in Ref. 11. The thermocouples were stretched horizontally (to minimize conduction errors) through holes burned in the glass tube and sealed in place with epoxy.

#### Theoretical Analysis:

Since the combustion process is steady, the gas and liquid phases were considered separately. However, phase equilibria requires the two solutions to match at the liquid surface.

The gas phase was treated by assuming an infinitely thin decomposition flame. The flame temperature and product gas concentration were determined from thermochemical calculations allowing for all relevant dissociation reactions. Data for these calculations was taken from the JANNAF Tables (3). The decomposition flame was assumed to be adiabatic in these calculations.

Two models were taken for phase equilibrium at the liquid surface. With the first model, high pressure corrections and ambient gas solubility were neglected. The mole fraction of fuel at the liquid surface was taken to be the ratio of the vapor pressure of the fuel at the surface temperature, to the total pressure in this model. The second, more complete model allowed for high pressure effects and the solubility of the combustion products in the liquid phase. While both models have been applied to the nitrate esters, only the low pressure model has been applied to the hydrazine data to date.

#### Results:

Work on the nitrate ester propellants was centered on resolving a discrepancy in the liquid surface temperatures for ethyl nitrate, between the present investigation and an earlier study by Hildebrand, et al (12). This involved retesting this fuel after the apparatus had been modified to improve measurement capabilities. These improvements included new camera optics for higher magnifications, a new synchronization system between the film and oscillograph records and improved background lighting. The results of retesting, following these improvements, were found to be in good agreement with earlier results of the present investigation.

A further check of the present results for the nitrate esters was obtained by analyzing plateau temperatures in addition to surface temperatures. During strand combustion, the thermocouple wire pulls a filament of liquid out of the surface, as the liquid burns past the thermocouple position. While this occurs, the liquid temperature rises above the true surface temperature and finally reaches a plateau temperature that is representative of a steady droplet burning condition (as the neck of the filament becomes small). These plateau temperatures were obtained from the thermocouple records of all the tests and compared with a modified version of the theory which allowed for the changed boundary conditions for steady droplet burning (as opposed to strand combustion). The agreement between the measured and predicted (high pressure theory) plateau temperatures

was found to be reasonably good. This indicates that the present surface and plateau temperatures are mutually consistent with one another. On this basis, it is now felt that the experimental results of Hildebrand, et al (12) are in error, although further testing by other investigators will probably be required to fully resolve the discrepancy.

The hydrazine fuels tested in the strand burner apparatus were hydrazine, MMH, and UDMH. However, MMH and UDMH failed to ignite and propagate for pressures up to 1000 psia, the highest pressure tested. Therefore, further testing with these fuels was abandoned. Hydrazine ignited and burned steadily from a pressure of 5 psia, the lowest pressure tested, to 300 psia. The upper limit for steady propagation is similar to the limit found by previous investigators (9, 13, 14).

A plot of the burning rate of hydrazine as a function of pressure is shown on Fig. 6. The burning rate was found to be linear with pressure. The results above 1 atm are similar to the results of Antoine (9) for 100% hydrazine in a 12.7 mm tube. The unusual burning rate behavior at various purities and tube sizes observed by Antoine for hydrazine was not encountered in the present investigation.

Figure 7 shows a plot of the boiling point curve for hydrazine along with the liquid surface temperatures predicted by the low pressure theory. Preliminary liquid temperature measurements indicated the need for modifying the apparatus in order to obtain accurate results for hydrazine. In the original apparatus, the thermocouple cold junction was located within the pressure vessel so that low cost heavy gage lead wires could be used to minimize electrical noise. While the heat sink at the cold junction was sufficient to maintain a constant cold junction temperature for the nitrate esters, this is not the case for hydrazine due to lower burning rates over the test range. In order to remedy this, a high pressure gland with 24 gage platinum - platinum 10% rhodium lead wires is being acquired so that the cold junction can be moved outside the apparatus. Upon the installation of this gland, the liquid temperature measurements will be completed for comparison with the theoretical results.

#### Summary and Conclusions:

Work on the nitrate ester fuels has been completed. The strand burning rates of hydrazine were measured in the pressure range of 5-300 psia. For pressures above atmospheric pressure, the strand burning rate of hydrazine varied linearly with pressure. Some liquid surface temperature measurements were made for hydrazine. However, these results were found to be in error since the cold junction was located inside the pressure vessel and it did not remain at a constant temperature during combustion.

The experimental apparatus is being modified to get the cold thermocouple junction outside of the pressure vessel. After this modification has been made, further testing will be done to obtain liquid surface temperature data for hydrazine. It is expected that this work will be completed early in the next report period.

#### IV. Oscillatory Combustion

##### Introduction:

High frequency combustion instability is a problem with liquid fueled rocket engines. The response of burning droplets to pressure and velocity oscillations is one component of the overall instability problem. Several theories have been developed to determine the response of liquids (15, 16). Other theoretical models consider the overall response of combustion chambers, treating the drop spray response as the controlling mechanism (17-19). However, present combustion instability data is limited to actual combustion chamber systems. Since this data deals with overall instability, the effect on instability of the response of burning drops is somewhat obscure.

The goal of this portion of the investigation is to study the response of a burning liquid surface to pressure oscillations. In particular, the response as a function of mean pressure and amplitude and frequency of the pressure oscillations is required. This data will provide a framework for comparing the various theories on the response of burning liquids. The experimental procedure involves observation of a burning liquid monopropellant strand subjected to pressure oscillations.

##### Experimental Apparatus:

The experimental apparatus must have the capability of varying the mean pressure, and the amplitude and frequency of the pressure oscillations and measuring the response of a burning liquid to these parameters. Fig. 8 is a sketch of the oscillatory combustion apparatus under development with the above capabilities. The major components of this apparatus are the glass tube filled with liquid monopropellant fuel, the camera used to measure the fluctuations of the burning liquid surface in response to the imposed pressure oscillations, and the rotary valve arrangement used to provide the oscillating pressure variations.

Two means of supplying the oscillating pressure were considered. One method used a piston-cylinder-rolling diaphragm arrangement. With this method the amplitude of the pressure oscillations could be varied by varying the stroke of the piston, and the frequency of the oscillations could be varied by varying the speed of the dynamometer used to drive the piston. Preliminary studies indicated that this system would be prohibitive in cost since a large power transmission system would be required.

The other method considered for supplying the oscillating pressure is sketched in Figure 8. This method is similar to the system described in Ref. 20 for establishing an oscillating propane gas flame. With this technique an oscillating pressure is set up in a test chamber by an oscillatory air stream. A stream of air is passed through a needle valve and ball valve mounted in parallel. The amplitude of the oscillatory pressure can be varied independently of the frequency by varying the relative amounts of air passing through the two valves. The frequency

of the oscillatory pressure is varied by varying the speed of the DC motor used to rotate the ball valve. The mean pressure in the chamber can be varied by the setting of the needle valve in the exhaust line.

Quasi-steady analysis indicates that the ability to optically resolve the oscillations of the liquid surface is the critical factor in the experimental technique. Fig. 9 is a plot of the amplitude of liquid oscillations versus the frequency of the imposed pressure oscillations for various imposed pressure amplitudes,  $P$ , for hydrazine. Also indicated are the critical frequencies (the critical frequency is defined as the characteristic frequency for transient liquid phase phenomena) for various mean pressures,  $P$ . In calculating the curves shown in Fig. 9, it was assumed that the burning rate of hydrazine varies linearly with pressure. The burning rate data obtained with the steady strand burner was used to evaluate the constants in the linear relation.

For the monopropellant strand system, the critical frequency is proportional to the burning rate squared divided by the liquid phase thermal diffusivity. Since the system behaves quasisteadily for pressure oscillation frequencies much less than the critical frequency, an important design requirement is to provide pressure oscillation frequencies in the range of the critical frequency in order to adequately test any transient response model.

It is evident from Fig. 9 that the conditions favoring large liquid surface oscillations (to facilitate measurement) are large pressure oscillations and low frequencies for a given total pressure. However, even for large pressure amplitudes and the frequencies of interest (near the critical frequency), the actual magnitude of the liquid surface oscillations is small.

The design of an optical system to resolve these small fluctuations is currently in progress. In addition, the components of the apparatus in Fig. 8 are being assembled. A review of the literature indicates that none of the current liquid surface response models provide for a monopropellant gas phase combustion process. Therefore, work is in progress to develop a transient response model for this case. The results with hydrazine on the flat flame burner indicate that this type of model would be more realistic for the hydrazine fuels under rocket engine conditions.

## V. High Pressure Droplet Combustion

### Introduction:

The main emphasis of this work centered on droplet burning in a cold gas environment at high pressures. For the experiments the droplet was simulated by a porous sphere with the liquid fuel being continuously admitted to the center of the sphere. Unlike the burning of droplets, where the process is mainly transient in nature, the burning porous fuel sphere may be considered to be a truly steady process. The experiments were conducted using ethanol, methanol, pentane, heptane, and decane

as the fuels. The pressure range was from 1 to 72 atmospheres. Objectives of these tests include the determination of burning rates at high pressures for a variety of fuels and the measurement of liquid surface temperature during steady combustion.

Theoretical analysis of this combustion process is also being undertaken. Several theoretical models are being considered including low and high pressure treatments of phase equilibrium as well as a number of methods of providing for gas phase property variations.

#### Experimental Apparatus:

A sketch of the experimental apparatus is shown in Fig. 10. The high pressure reactor is provided with quartz windows for observing the combustion of the porous sphere. The reactor is of steel construction and lined with alumina fire-brick.

Air for the combustion process is supplied by a 3000 psia compressor which is accurately controlled by a critical flow jeweled orifice system, of the type described by Anderson and Friedman (21). The reactor pressure and the pressure upstream of the orifices is measured with Heisse Bourdon tube gages.

The hot exhaust gases leaving the reactor are cooled in a water cooled concentric tube heat exchanger. Water condensed in the heat exchanger is collected in a water trap and periodically blown off to a drain. The reactor pressure is controlled by a regulating valve in the exhaust line. After passing through the regulating valve, the reactor gases are exhausted to the atmosphere. The emergency pressure release system consists of a rupture disk assembly set at 2000 psia.

The porous spheres used in the combustion tests are made of alundum. A sketch of a fuel probe is shown in Fig. 11. The fuel is fed to the center of the sphere through a stainless steel water cooled tube. Referring to Fig. 11, the fuel is introduced through the center tube while coolant water passes through the second innermost tube and leaves through the annulus formed by the second and third tubes. The outside diameter of the cooled fuel feed line is 0.317 cm; the minimum sphere diameter is 0.95 cm.

Liquid temperatures at the surface of the sphere are measured using two 0.0076 cm diameter chromel-alumel thermocouples. The thermocouples are mounted on the sphere such that the junction of the thermocouple is flush with the surface. The thermocouples are cemented in place and located approximately 60 degrees apart along the periphery of the sphere.

The fuel is pumped to the center of the sphere using a Whitey precision pump with a 10 mm plunger. The pump has a maximum discharge pressure 5000 psia and a maximum delivery rate of 2200 milliliters per minute.

Burning rates are determined by measuring the time it takes for a given quantity of fuel to be consumed. The liquid volume measurements are made with a graduated burette located at the inlet of the pump. Steady state burning is achieved when the sphere is completely wet but not dripping.

## Theoretical Analysis:

The theoretical analysis of this system may be divided into a gas phase model of the combustion process and a phase equilibrium model for conditions at the liquid surface. Several gas phase models are being investigated. The most complete gas phase model involved an extension of the analysis given by Lazar and Faeth (23), for high pressure, quasi-steady droplet combustion. The extension involved allowing for the effect of natural convection as well as changes due to the differing boundary conditions at the liquid surface for the present experiment. This analysis allows variable thermal conductivity and binary diffusivities on both sides of the bipropellant diffusion flame around the porous sphere with variable specific heats for all species. A simplified version of this analysis is also being considered which assumes constant specific heats, but in all other respects is similar to the more complex model. Finally, a constant property analysis is being employed for comparison with the two variable property gas phase models.

Several models of increasing complexity are also being employed to compute phase equilibrium at the liquid surface. The simplest model neglects real gas effects and solubility and is analogous to the models used in early studies of high pressure droplet combustion. In the more complex models, real gas effects are considered through the use of a modified Redlich-Kwong equation of state with mixing rules similar to those employed in Ref. 22. For combustion in air, the major gaseous species at the liquid surface are the fuel vapor, nitrogen, carbon dioxide and water vapor. Since nitrogen predominates the non-fuel species in this system, a simplified version of the high pressure model assumes that the gas mixture can be represented by a binary mixture of fuel and nitrogen. The most complete phase equilibrium model considered the quaternary system; fuel, nitrogen, carbon dioxide and water.

## Results:

The fuels tested to date consisted of three hydrocarbons (pentane, heptane, and decane) and two alcohols (methanol and ethanol). The alcohols were tested from 1 to 72 atmospheres and the hydrocarbons from 1 to about 50 atmospheres. Repeatability was good for the fuels tested except at relatively low pressures (1 to 4 atmospheres) where some scatter was observed.

Plots of the burning rate data versus pressure are shown in Figs. 12 and 13. These results show a fairly linear increase in burning rate with pressure on logarithmic coordinates. The increase in burning rate with pressure is largely attributable to natural convective effects.

Experimental observations included observation of sooting with the hydrocarbon fuels. Sooting was first observed around 7 atmospheres for decane and heptane and around 6 atmospheres for pentane. With the exception of the alcohols all fuels exhibited high flame luminosity. This trend also started around 7 atmospheres. Methanol burned with a pale blue flame that tended to yellow at high pressures. The ethanol flame was yellowish throughout the pressure range tested. Excessive carbon formation was noted with ethanol around 1100 psia.

The calculated results are not complete at this time, however, preliminary results indicate fair agreement between theoretical and experimental burning rates. In general, the rate of increase of the burning rate with pressure is somewhat overestimated by the theories. This behavior is possibly due to decomposition effects associated with the formation of soot at high pressures. A more detailed discussion of these results will be deferred until all calculations are complete.

#### Summary and Conclusions:

Collection of the burning rate and liquid temperature data is continuing in the upper pressure range (from 50 to 100 atmospheres). A third alcohol, propanal, will also be tested and some testing will also be done with larger spheres. For each fuel a series of dark field photographs will be taken of the combustion process to indicate flame diameters, appearance, etc. Calculations using the theoretical model are in progress. It is expected that this work on fuel droplet combustion in a cold gas environment will be completed early in the next report period.

### VI. High Pressure Flat Flame Study

#### Introduction:

The flat flame burner system was designed to provide a more realistic burning atmosphere for the porous spheres than is the case for the cold gas tests. In conjunction with the high-pressure combustion apparatus, conditions simulating those of a typical combustion process can be achieved. The burner used in the tests employed a premixed flame supplied with a mixture of nitrogen, carbon monoxide, and oxygen.

The premixed flat flame burner used in the tests was found to be limited to relatively low pressure applications. In order to achieve the desired range of pressures, a diffusion flame burner is currently under development. One of the most important advantages of the diffusion flame burner is the elimination of flashback, a problem inherent in burners of the premixed flame type. Also, the diffusion burner leads itself to a much simpler design. In the diffusion burner tests, in addition to carbon monoxide, methane will also be used as a burner fuel gas.

#### Experimental Apparatus:

The premixed flat flame burner (Fig. 14) is constructed of stainless steel and brass. The major components of the burner consist of the burner base, a water coolant assembly, and a nitrogen diluent system. The flame is stabilized as a thin flat reaction zone located a short distance above the porous plate. The main purpose of the nitrogen diluent system was to provide flame stability and a more uniform flow field past the test position. Tests indicated that the diluent lessened the tendency of the flame to lift from the burner plate. The mixing chamber is filled with steel wool and fine wire gauze. A layer of copper shot is used to conduct heat from the base of the sintered bronze porous burning plate to the copper cooling coil. The burner plate is 2 inches in diameter. The

principal fuel used with this burner was technical grade carbon monoxide in combination with various mixtures of oxygen and nitrogen.

#### Results:

The premixed flat flame burner was tested at pressures up to 4 atmospheres. Over this pressure range a wide variety of mixture ratios were used. Testing revealed that a slightly fuel-rich flame proved to be the most stable over the pressure range. Unfortunately, at pressures in excess of 4 atmospheres the flame would occasionally flashback past the burner plate. Since repeated attempts to remedy this problem proved unsuccessful, it was decided to switch to a diffusion flame burner which is fundamentally incapable of flashback. A sketch of the new burner with modifications tailored to high pressure combustion is shown in Fig. 15. The design of this burner is patterned after the multiple diffusion burner developed by Berl and Wilson (22). For this design, stainless steel capillary tubing of 0.035 inch outside diameter separated by thin metal shims is used instead of the porous metal plate used in the premixed burner. The flow areas of the fuel and oxidizer inlets are proportioned to provide the proper mixture ratios and gas velocity ratios. The capillary tubing is silver brazed to the base of the burner.

The coolant system and nitrogen diluent system will be similar to those on the premixed flat flame burner. The principal fuel for the diffusion burner will be methane. Critical flow orifices will be used to provide accurate flow control.

#### Summary and Conclusions:

Upon completion of the cold gas tests, experimentation will begin using the flat flame burner. The same type of tests will be run except a high temperature variable composition and variable velocity environment will be provided to simulate combustion chamber conditions. The pressure range of these tests will be from 1 to 100 atmospheres with fuels similar to those considered in the cold gas testing.

## References

1. Allison, C. B. and Faeth, G. M., "Hybrid and Decomposition Combustion of Hydrazine, MMH and UDMH as Droplets", Eighth JANNAF Liquid Propellant Combustion Instability Meeting, Aerospace Corp., Los Angeles, California, October, 1971.
2. Allison, C. B., "Hybrid and Decomposition Combustion of the Hydrazine Fuels", NASA CR-72977, July 1971.
3. Jones, W. H. (Chairman), JANNAF Thermochemical Tables, Dow Chemical Company, Midland, Michigan.
4. Spalding, D. B. and Jain, V. K., "Theory of the Burning of Monopropellant Droplets", A.R.C. Technical Report No. 20-176, Current Paper No. 447, 1958.
5. Dykema, O. W. and Greene, S. A., "An Experimental Study of RP-1, UDMH, and  $N_2H_4$  Single Droplet Burning in Air and Oxygen", Liquid Rockets and Propellants, Progress in Astronautics and Rocketry, Vol. 2, Academic Press, New York, 1960, pp. 299-324.
6. Rosser, W. A., Jr., "The Decomposition Burning of Monopropellant Drops: Hydrazine, Nitromethane, and Ethyl Nitrate", Progress Report No. 20-305, Jet Propulsion Laboratory, Pasadena, California, January 1957.
7. Lawver, B. R., Kosvic, T. C., and Breen, B. P., "Effects of Additives on the Combustion of Hydrazine", AFRPL-TR-67-288, January, 1968, Dynamic Science Corporation, Monrovia, California.
8. Kosvic, T. C., and Breen, B. P., "Study of Additive Effects on Hydrazine Combustion and Combustion Instability at High Pressure", AFRPL-TR-69-12, November, 1969, Dynamic Science Corporation, Monrovia, California.
9. Antoine, A. C., "The Mechanism of Burning of Liquid Hydrazine", Eighth Symposium (International) on Combustion, Williams and Wilkins, Baltimore, 1962, pp. 1057-1059.
10. Faeth, G. M., "High Pressure Liquid Monopropellant Combustion", to be published in Combustion and Flame.
11. Fristrom, R. M. and Westenberg, A. A., Flame Structure, McGraw-Hill Book Company, New York, 1965, pp. 170-174.
12. Hildebrand, D. L., Whittaker, A. G., and Euston, C. B., "Burning Rate Studies I. Measurement of the Temperature Distribution in Burning Liquid Strands", J. Phys. Chem., Vol. 58, 1954, pp. 1130-1133.
13. Adams, G. K. and Stocks, G. W., "The Combustion of Hydrazine", Fourth Symposium (International) on Combustion, Williams and Wilkins, Baltimore, 1953, pp. 239-248.

14. Gray, P. and Kay, J. C. "Stability of the Decomposition Flame of Liquid Hydrazine", Research, London, Vol. 8, 1955, pp. 53-55.
15. Heidmann, M. F. and Wieber, P. R., "Analysis of Frequency Response Characteristics of Propellant Vaporization", AIAA Paper No. 66-604, 1966.
16. T'ien, J. S. and Sirignano, W. A., "Unsteady Thermal Response of the Condensed Phase Fuel Adjacent to a Reacting Gaseous Boundary Layer", Thirteenth Symposium (International) on Combustion, The Combustion Institute, Pittsburgh, Penna., 1971, pp. 529-539.
17. Beltran, M. R., et al, "Analysis of Liquid Rocket Engine Combustion Instability", Technical Report No. AFRPL-TR-65-254, Dynamic Science Corporation, Monrovia, California, 1966.
18. Kosvic, T. C. and Breen, B. P., "Study of Additive Effects on Hydrazine Combustion and Combustion Instability at High Pressures", Technical Report No. AFRPL-TR-69-12, Dynamic Science Corporation, Monrovia, California, 1968.
19. Lawver, B. R., Kosvic, T. C. and Breen, B. P., "Effect of Additives on the Combustion of Hydrazine", Technical Report No. AFRPL-TR-67-299, Dynamic Science Corporation, 1968.
20. Chervinsky, A. P., Sirignano, W. A., Harrje, D. T., and Varma, A. K., "Axisymmetric Jet Diffusion Flame in an External Oscillating Stream", Sixth ICRPG Combustion Conference, CPIA Publication No. 192, December 1969.
21. Anderson, J. W. and Friedman, R., "An Accurate Metering System for Laminar Flow Studies," The Review of Scientific Instruments: Vol. 20, No. 1, Jan. 1940, p. 66.
22. Berl, W. G., and Wilson, W. E., "Formation of BN in  $B_2H_6-N_2H_4$  Flames," Nature, 191, 380 (1961).
23. R. S. Lazar and G. M. Faeth, "Bipropellant Droplet Combustion in the Vicinity of the Critical Point," Thirteenth Symposium (International) on Combustion, The Combustion Institute, Pittsburgh, Pennsylvania, 1971, pp. 743-753.
24. R. S. Lazar and G. M. Faeth, "Gas Solubility Effects During High Pressure Liquid Propellant Combustion," Proceedings of the 7th JANNAF Liquid Combustion Instability Meeting, CPIA Publication 204, Vol. 1, February 1971, pp. 543-552.
25. G. M. Faeth and R. S. Lazar, "Fuel Droplet Burning Rates in a Combustion Gas Environment," AIAA J., Vol. 9, No. 11, 1971, pp. 2165-2171.

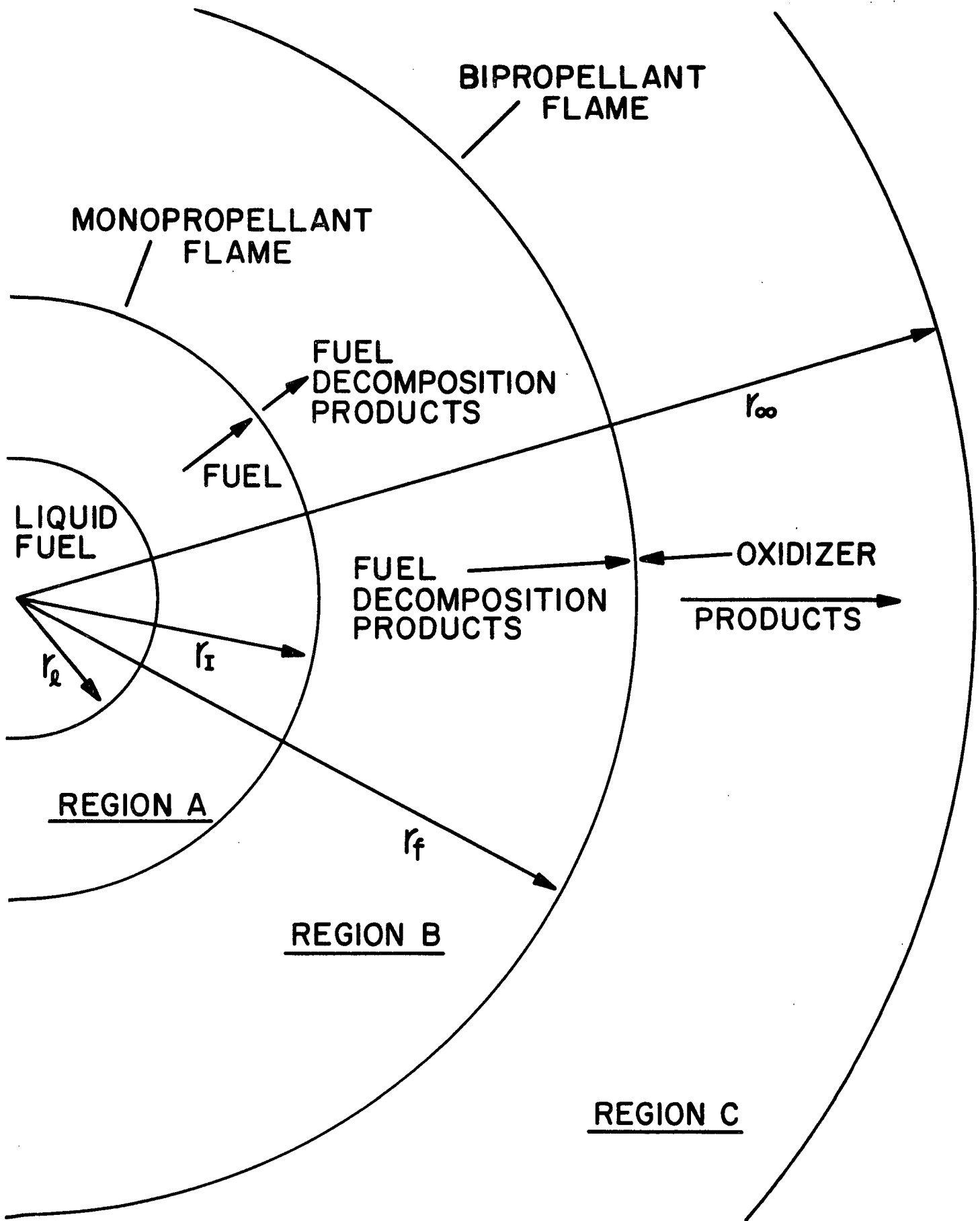


Fig. 1 Sketch of the hybrid combustion model.

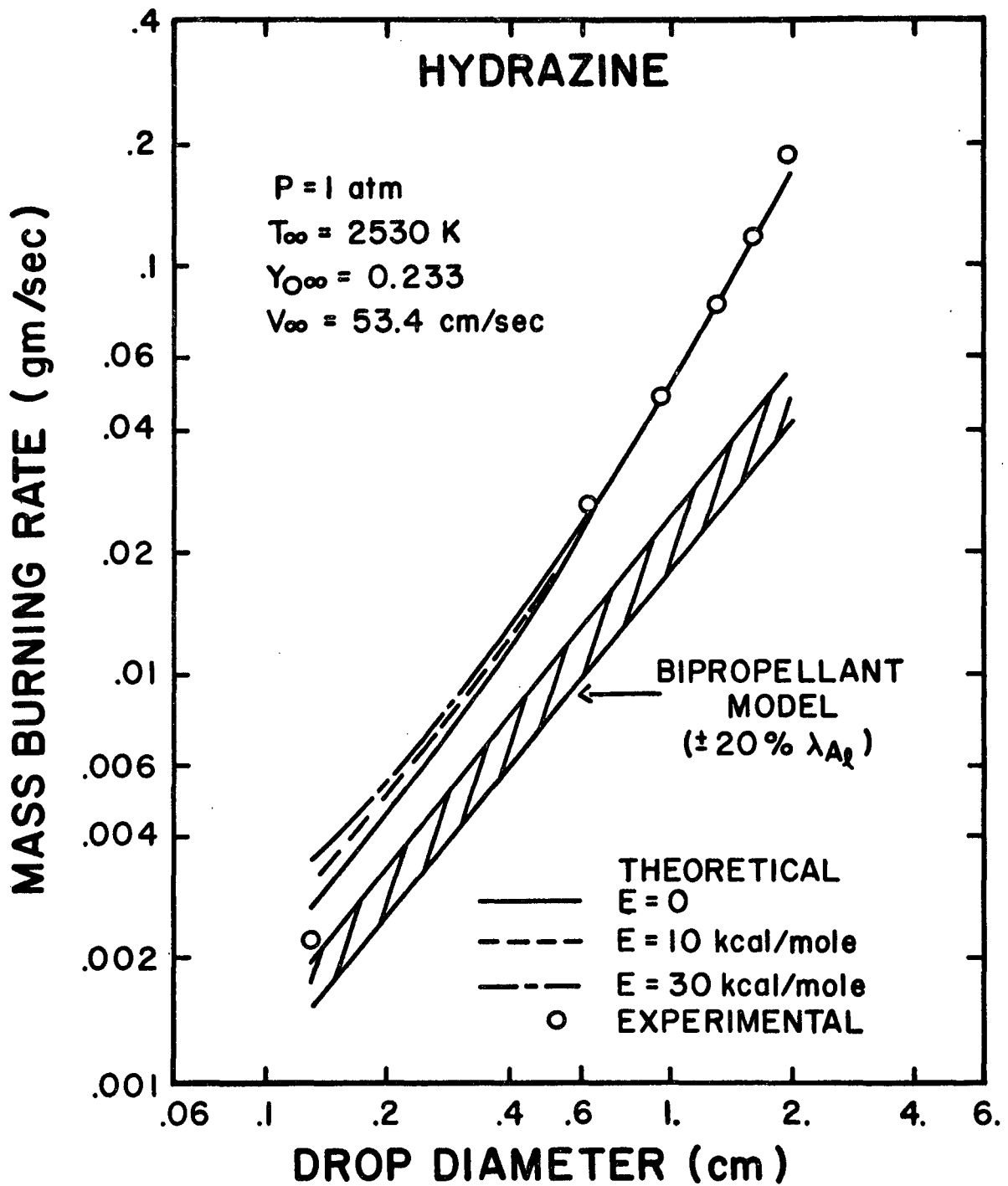


Fig. 2 Hydrazine burning rates as a function of drop diameter for a typical oxidation condition.

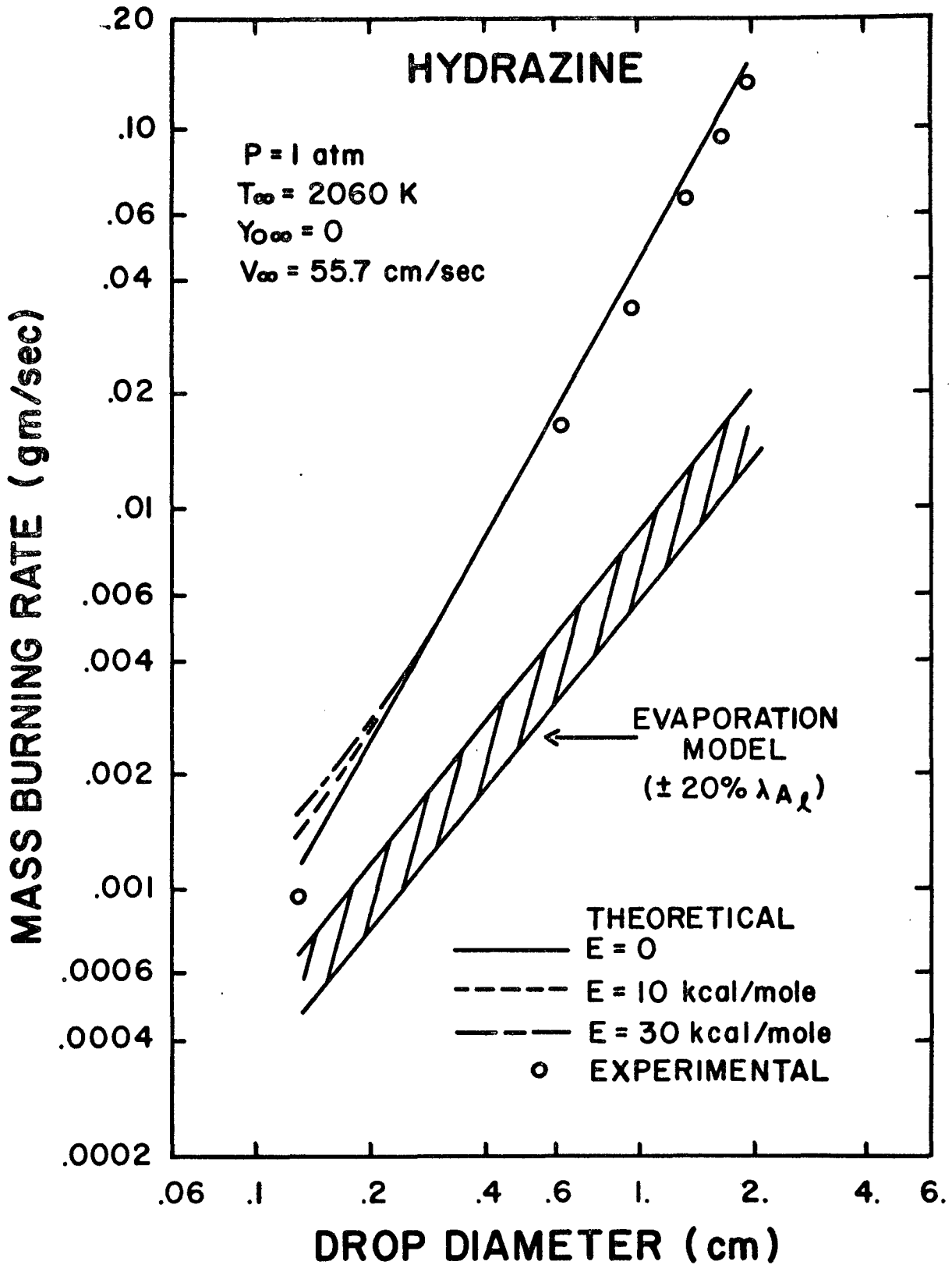


Fig. 3 Hydrazine burning rates as a function of drop diameter for a typical decomposition condition.

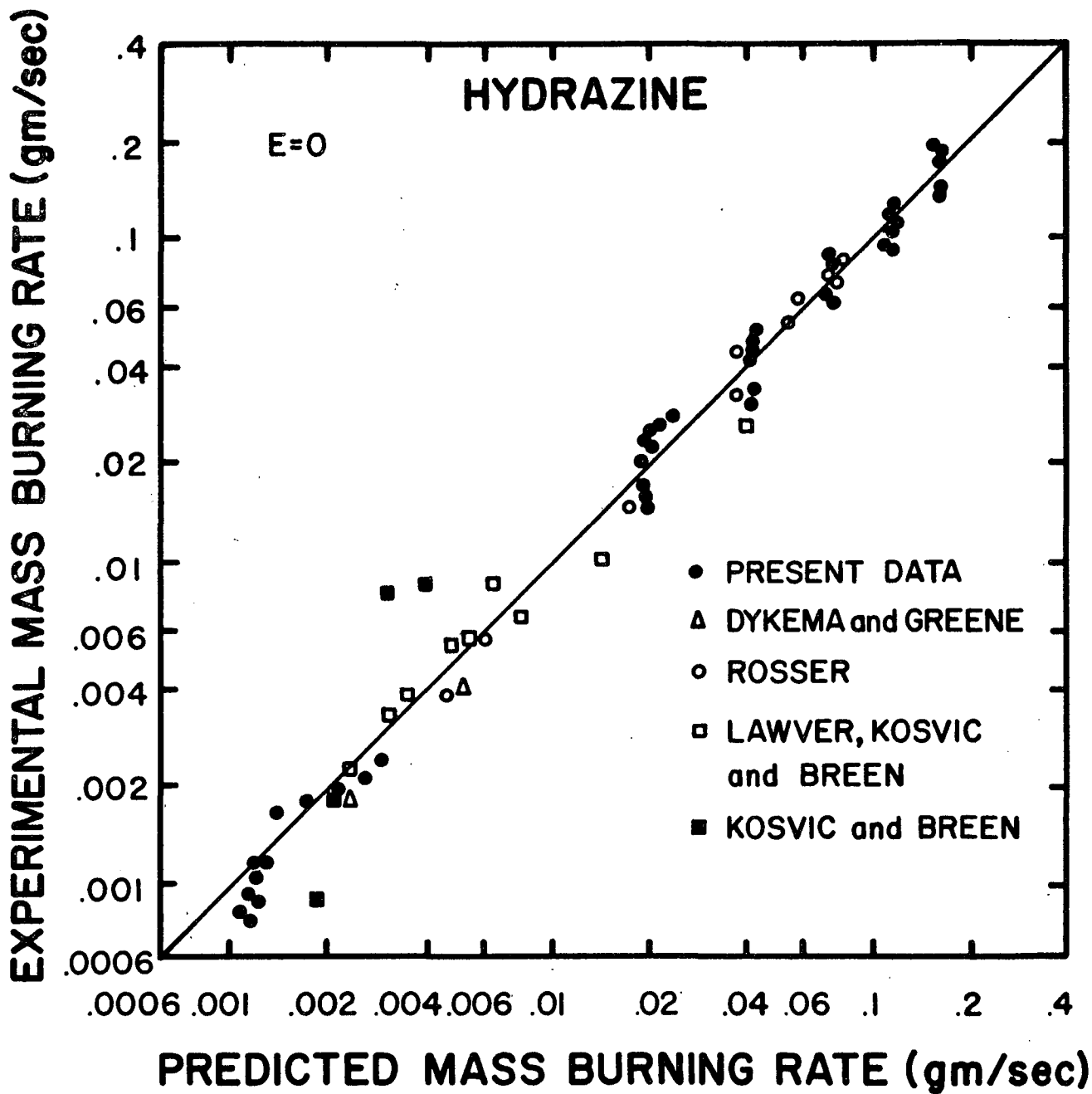


Fig. 4. Comparison of experimental and predicted burning rates for hydrazine.

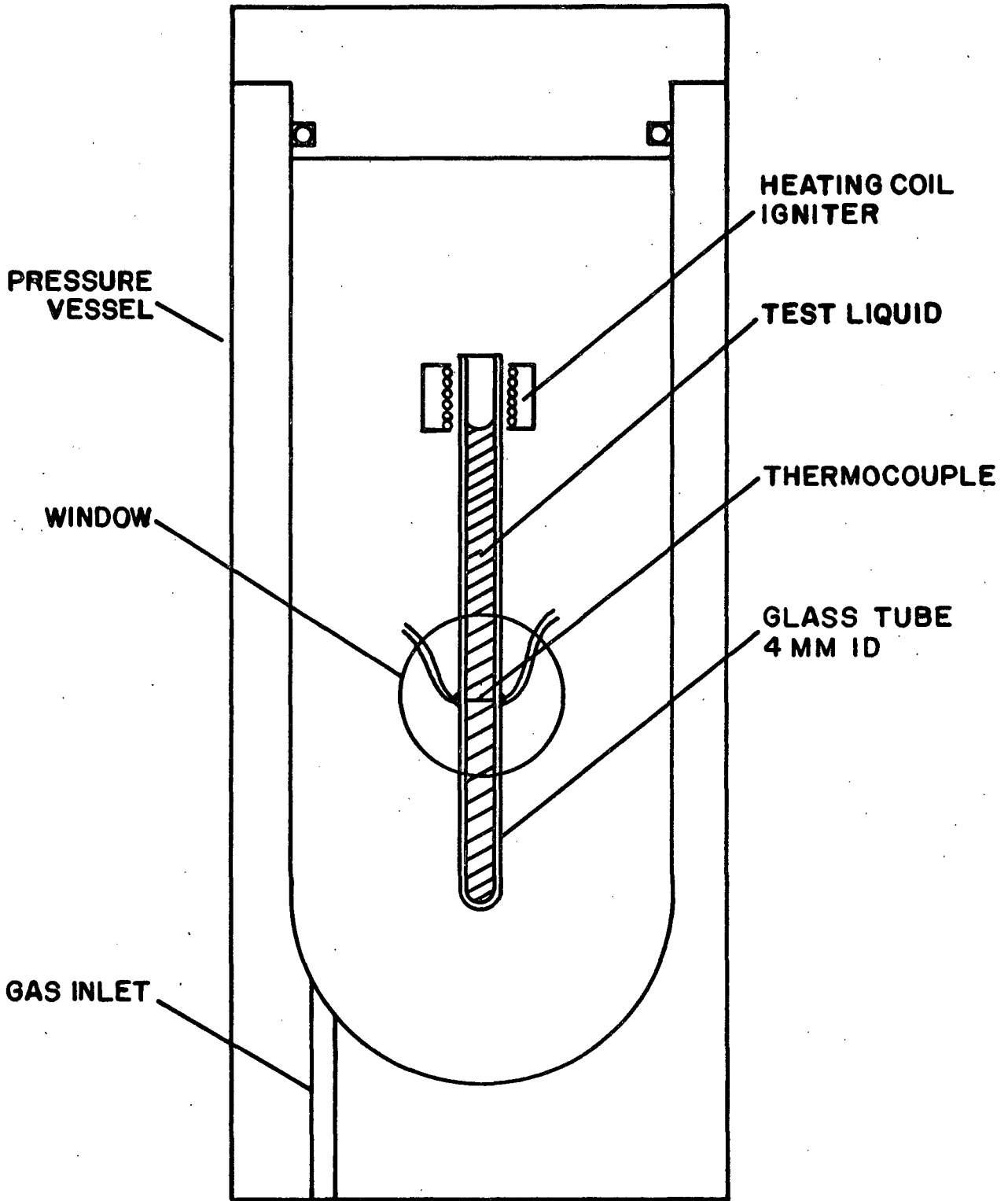


Fig. 5. Sketch of the strand burner apparatus.

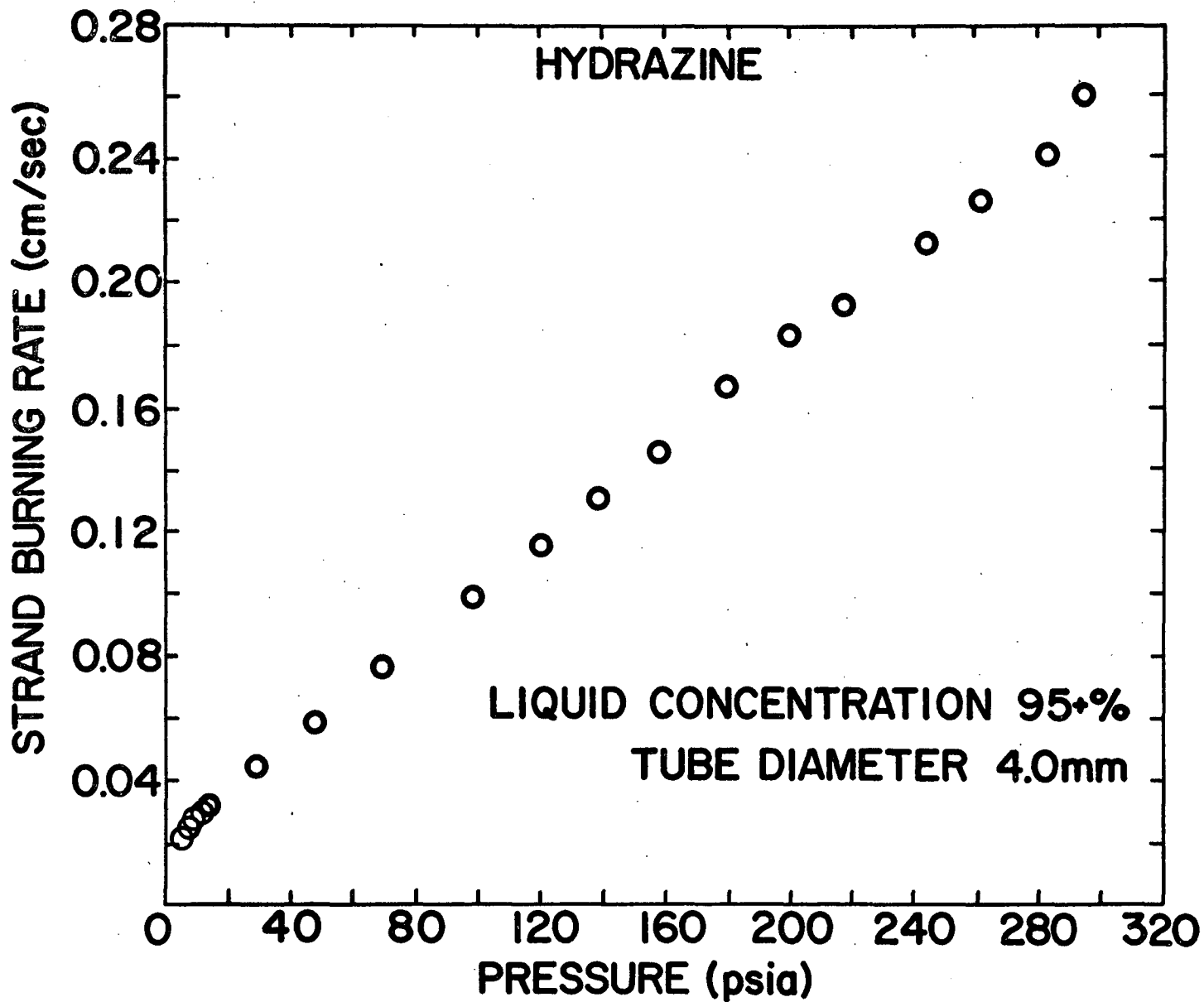


Fig. 6 Hydrazine strand burning rates as a function of pressure.

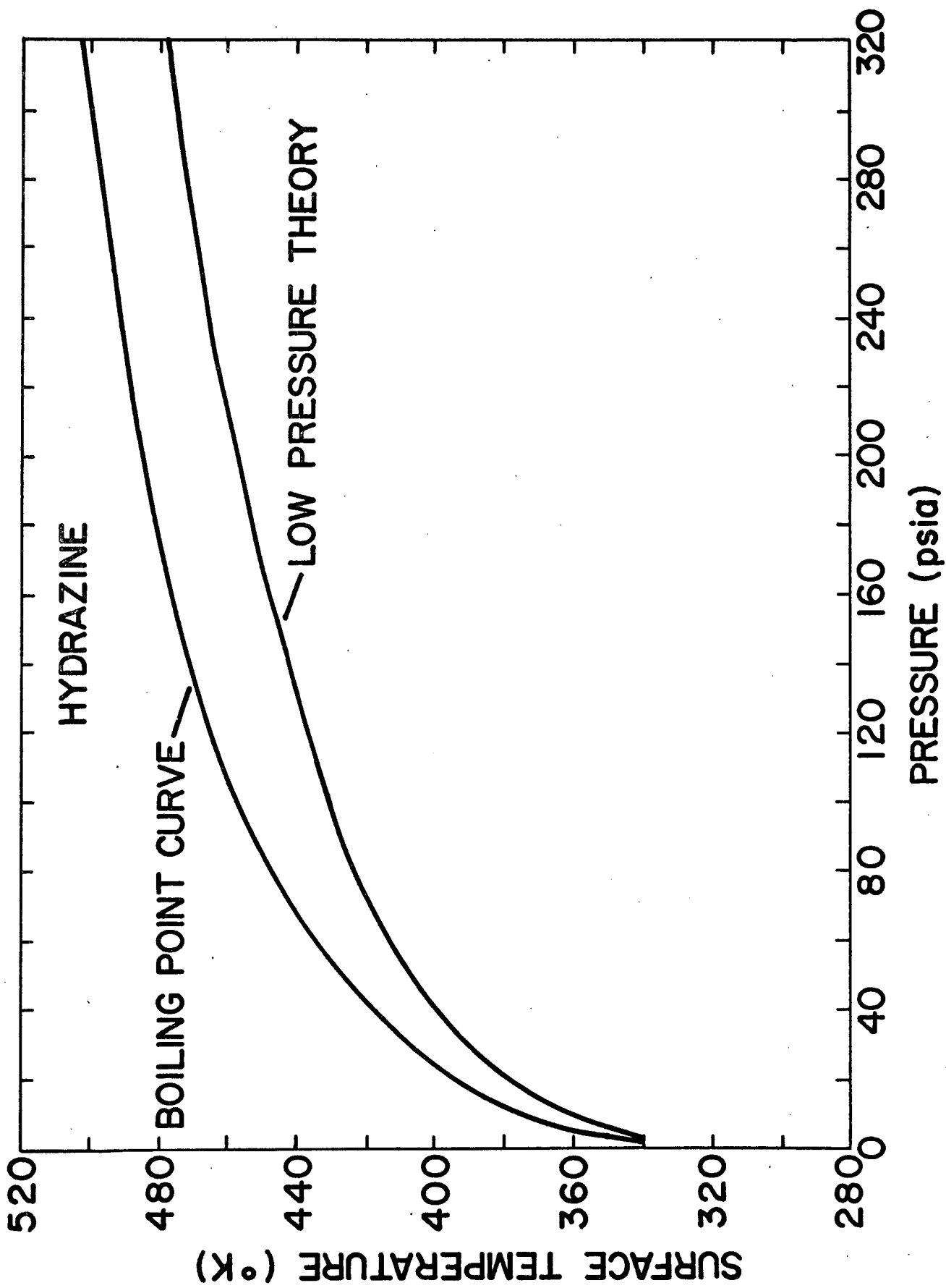


Fig. 7 Hydrazine surface temperatures as a function of pressure.

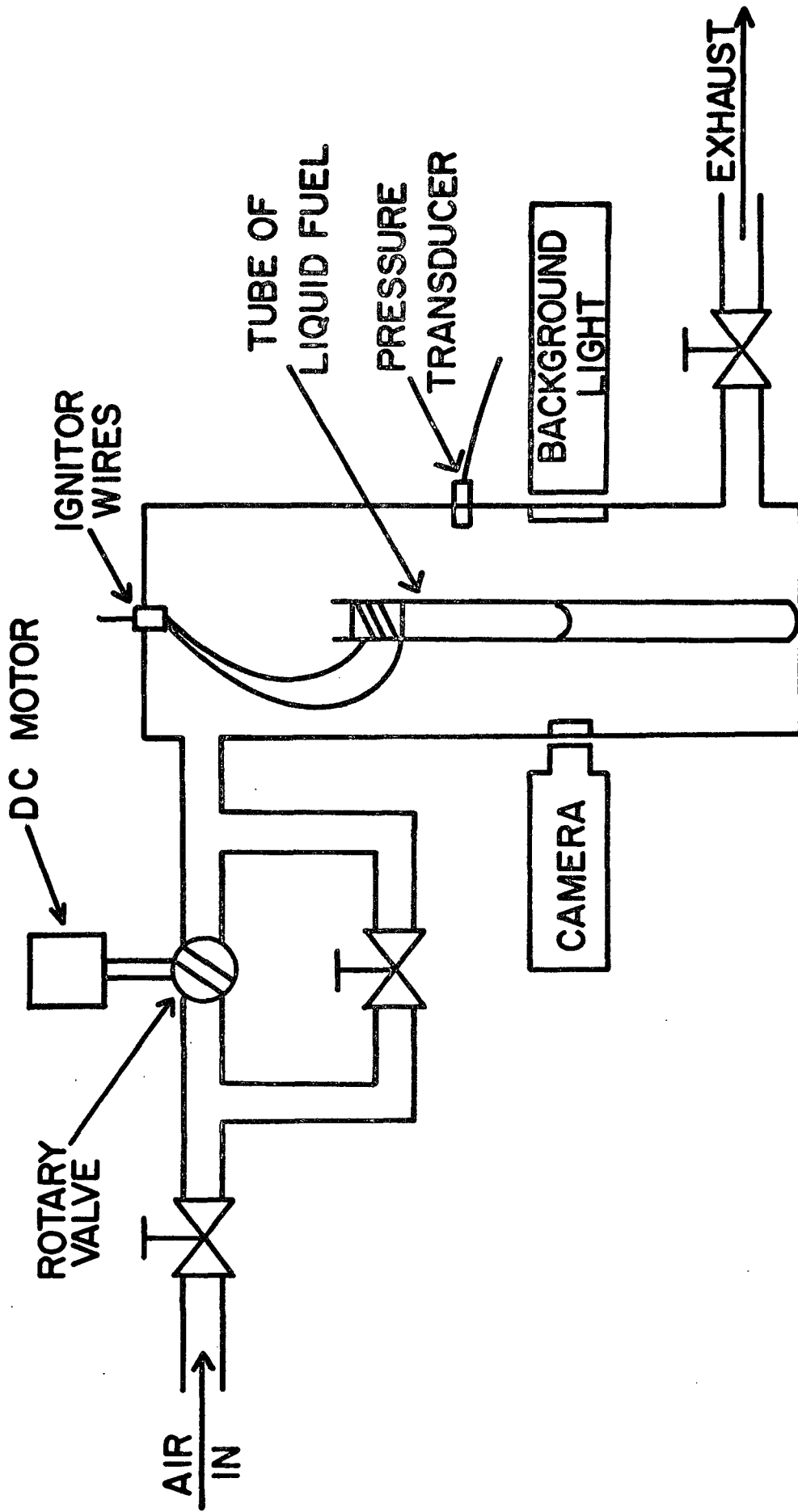


Fig. 8 Sketch of the oscillatory combustion apparatus.

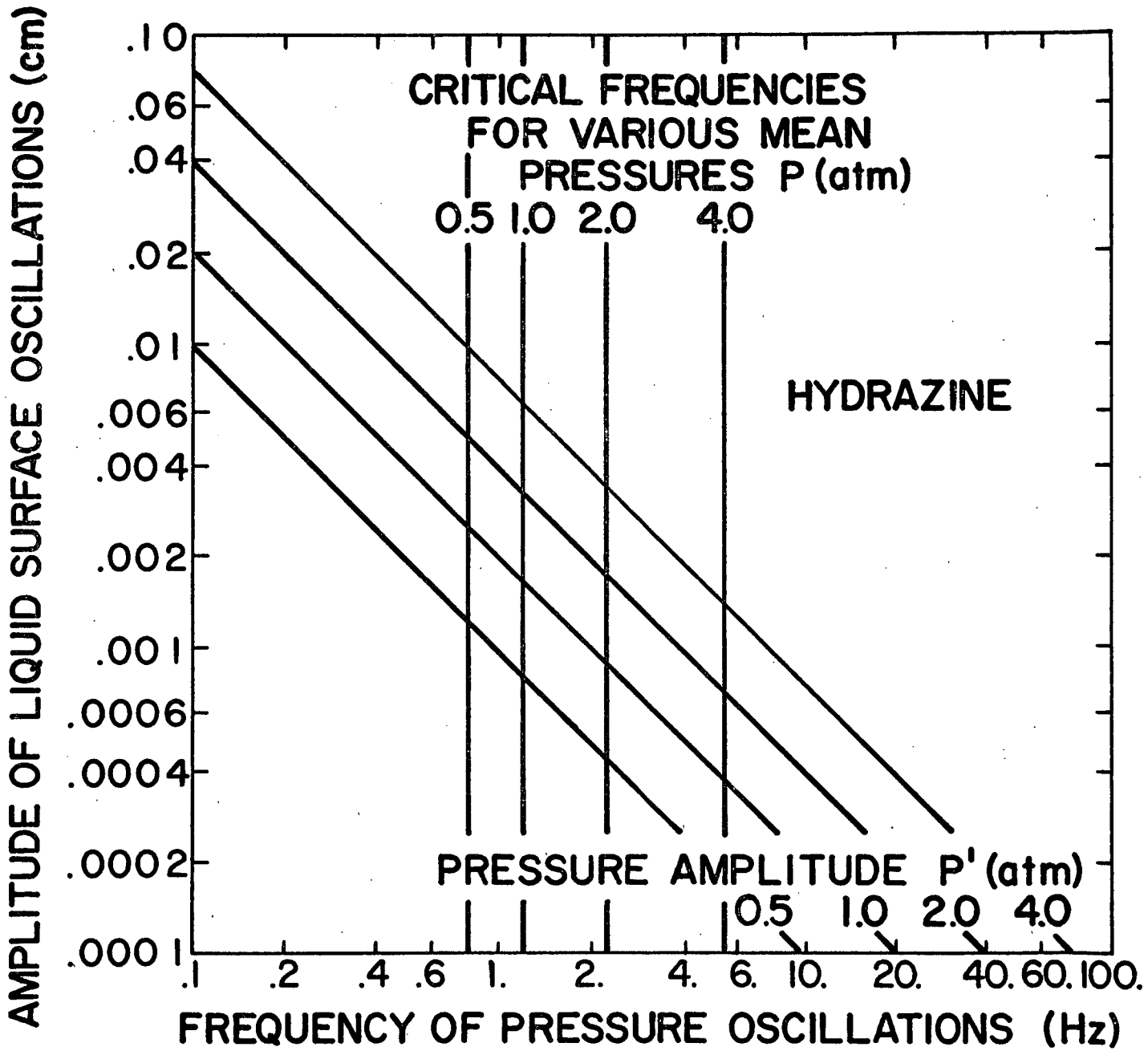


Fig. 9 Quasi-steady response of liquid hydrazine to imposed pressure oscillations.



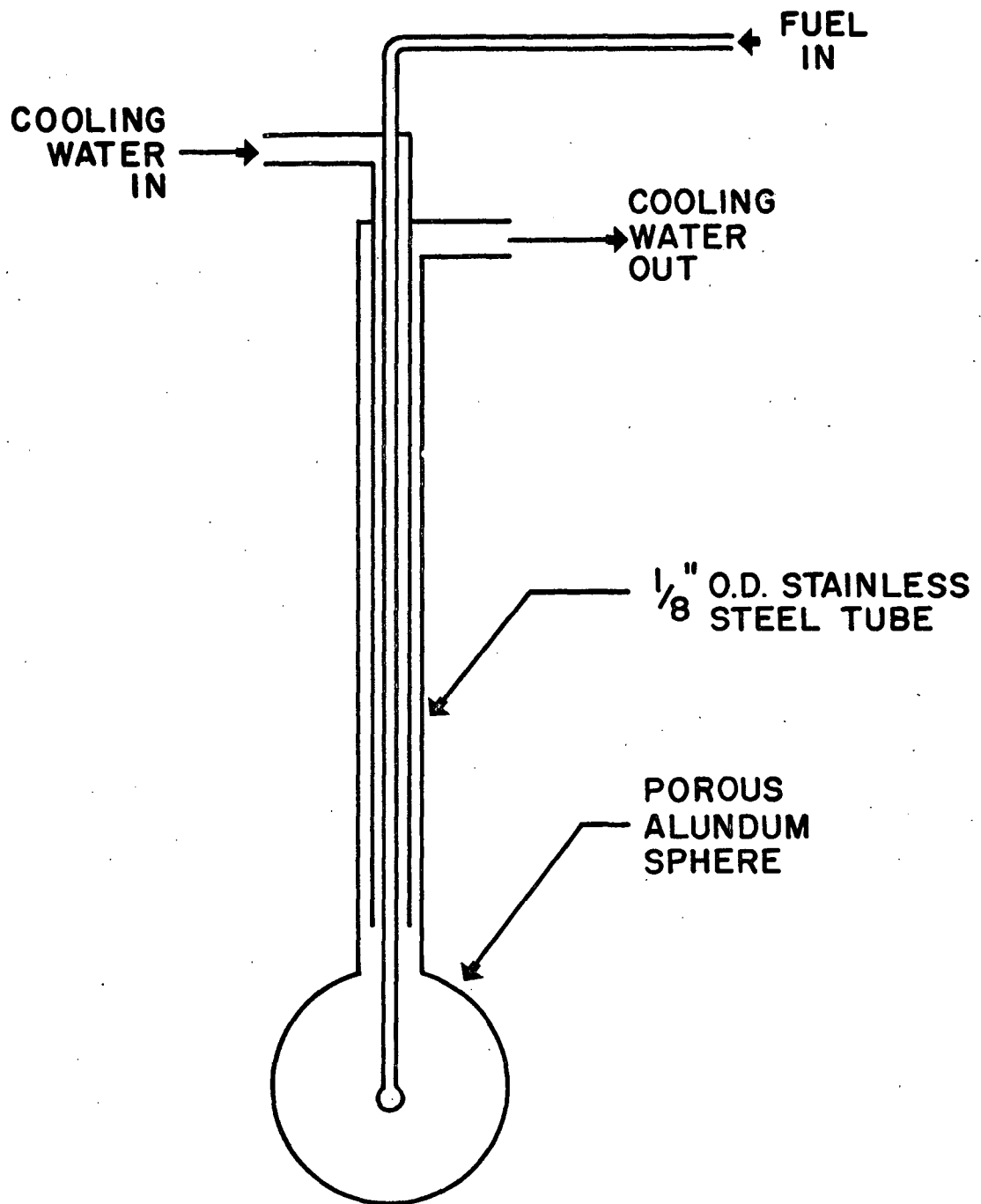


FIG. II POROUS SPHERE PROBE

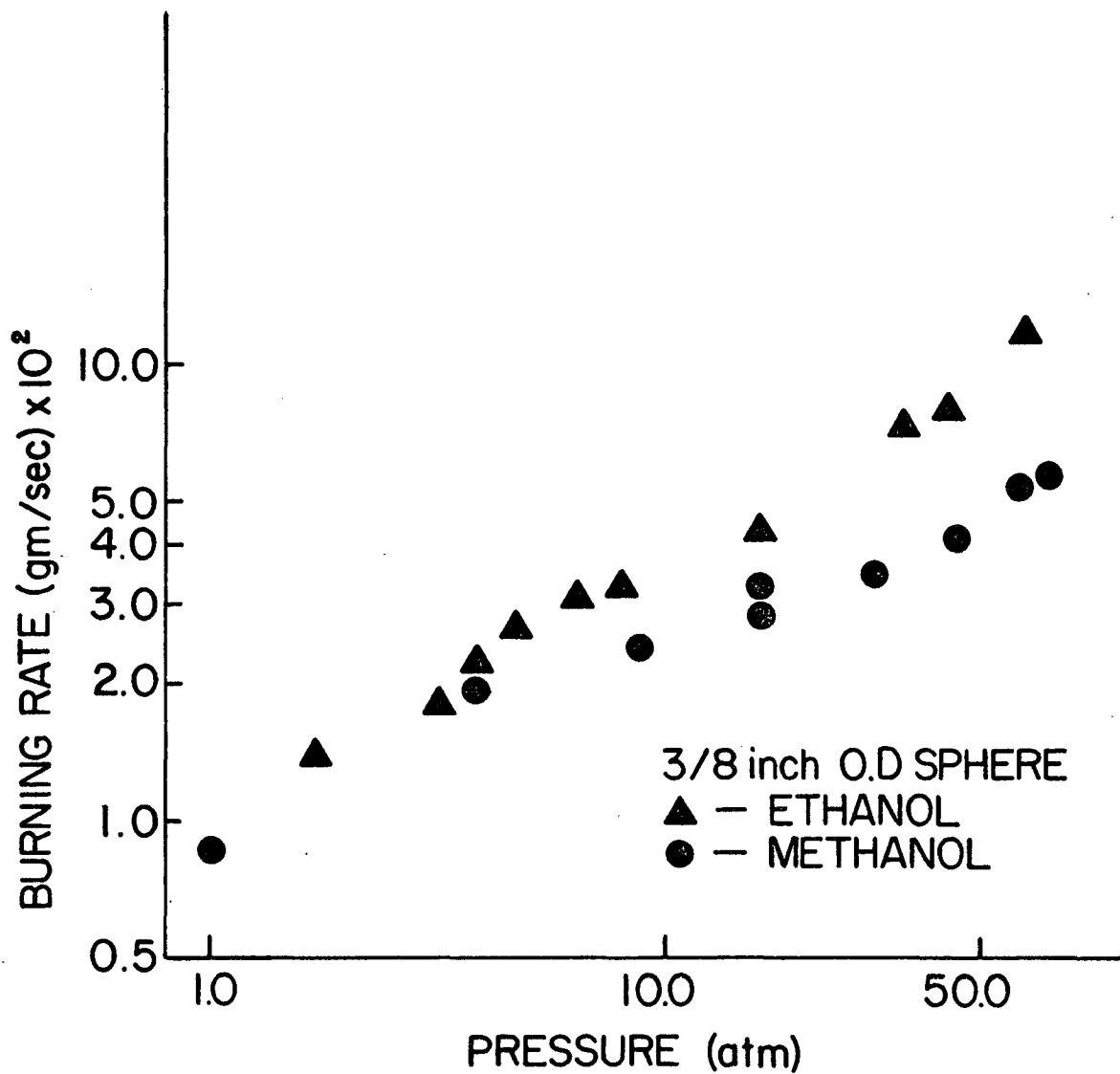


Fig. 12 High pressure burning rates of alcohols.

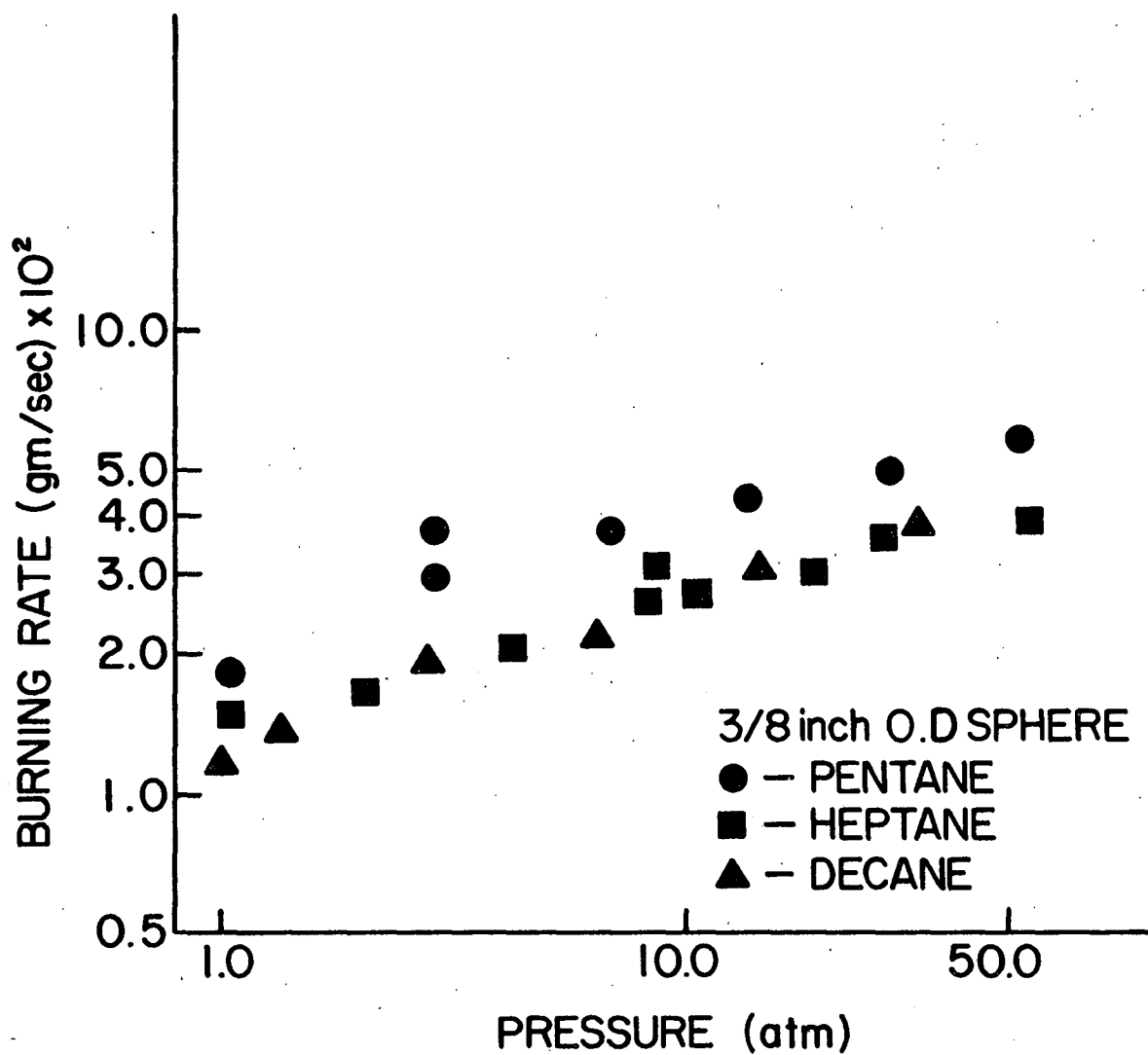
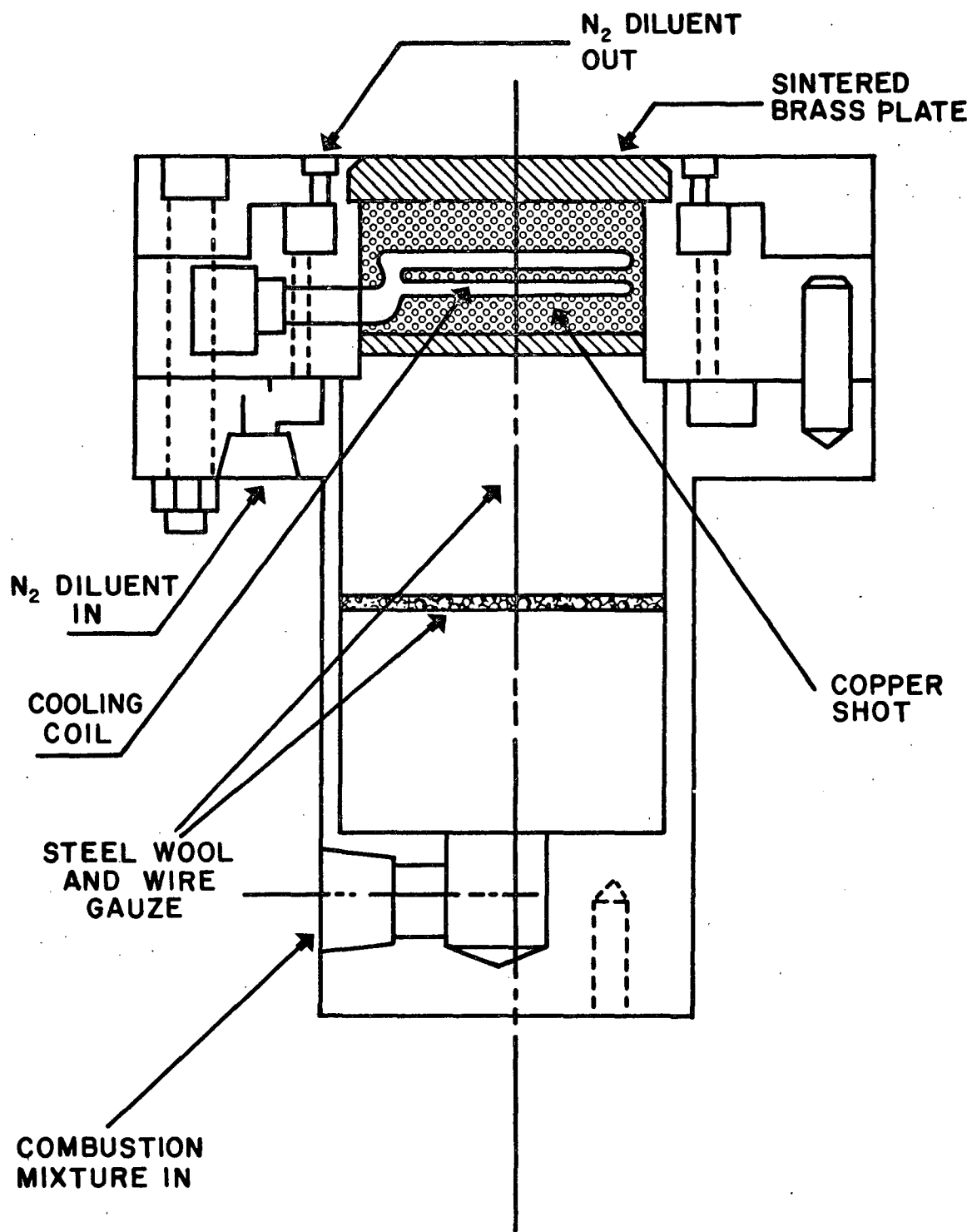


Fig. 13 High pressure burning rates of paraffins.



**FIG. 14 HIGH PRESSURE FLAT FLAME BURNER**

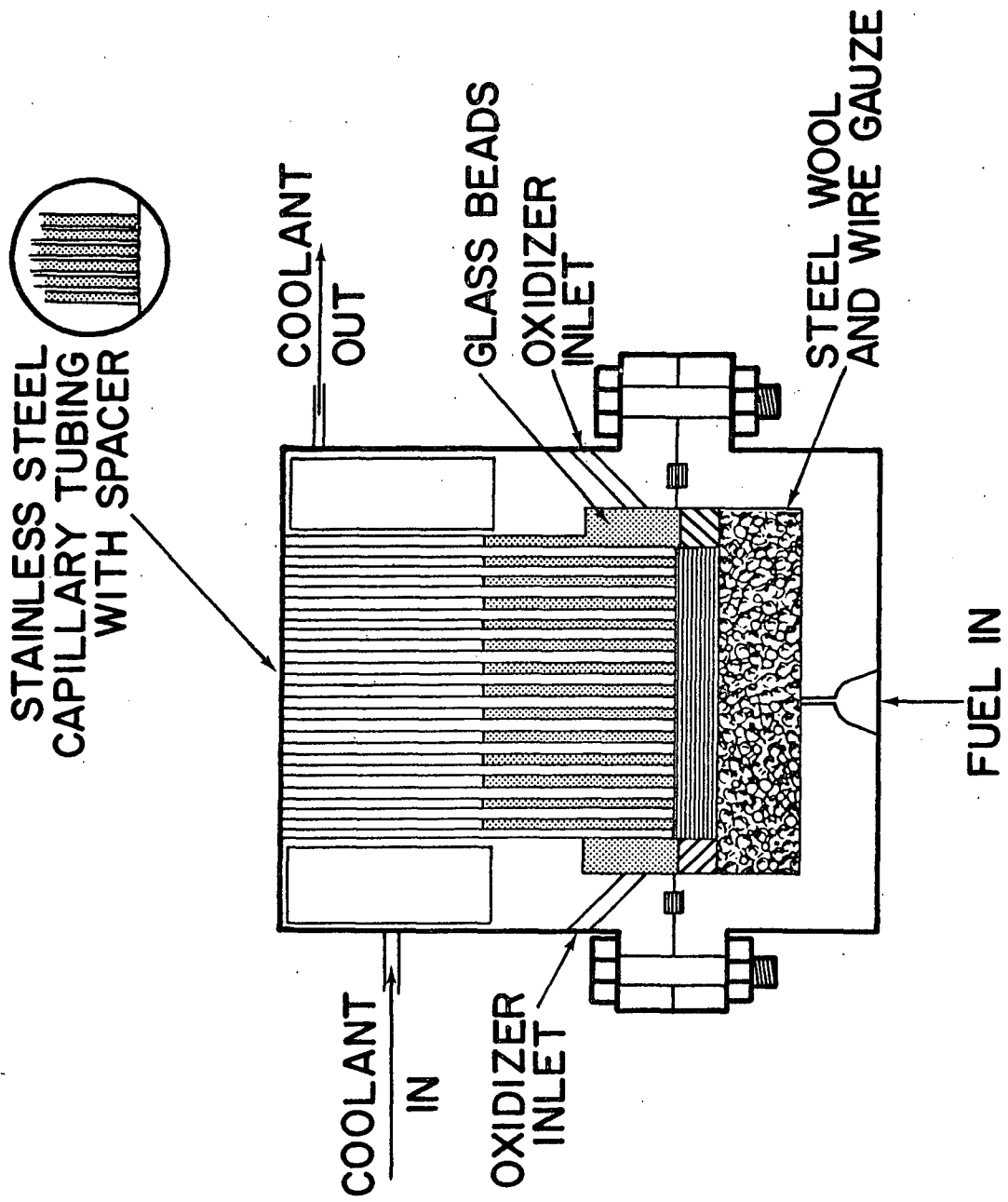


FIG.15 DIFFUSION FLAME BURNER

REPORT DISTRIBUTION LIST OF CONTRACT NO. NGR 39-009-077

Dr. R. J. Priem MS 500-204  
NASA Lewis Research Center  
21000 Brookpark Road  
Cleveland, Ohio 44135 (2)

Norman T. Musial  
NASA Lewis Research Center  
21000 Brookpark Road  
Cleveland, Ohio 44135

Library (2)  
NASA Lewis Research Center  
21000 Brookpark Road  
Cleveland, Ohio 44135

Report Control Office  
NASA Lewis Research Center  
21000 Brookpark Road  
Cleveland, Ohio 44135

Brooklyn Polytechnic Institute  
Attn: V. D. Agosta  
Long Island Graduate Center  
Route 110 Farmingdale, New York 11735

Chemical Propulsion Information Agency  
Johns Hopkins University/APL  
Attn: T. W. Christian  
8621 Georgia Avenue  
Silver Spring, Maryland 20910

NASA Lewis Research Center  
Attn: E. W. Conrad, MS 500-204  
21000 Brookpark Road  
Cleveland, Ohio 44135

North American Rockwell Corporation  
Rocketdyne Division  
Attn: T. A. Coultas, D/991-350  
Zone 11  
6633 Canoga Avenue  
Canoga Park, California 91304

National Technical Information Service  
Springfield, Virginia 22151  
(40 copies)

NASA Representative  
NASA Scientific and Technical  
Information Facility  
P. O. Box 33  
College Park, Maryland 20740  
(2 copies with Document Release  
Authorization Form)

Aerospace Corporation  
Attn: O. W. Dykema  
Post Office Box 95085  
Los Angeles, California 90045

Ohio State University  
Department of Aeronautical and  
Astronautical Engineering  
Attn: R. Edse  
Columbus, Ohio 43210

TRW Systems  
Attn: G. W. Elverum  
One Space Park  
Redondo Beach, California 90278

Bell Aerospace Company  
Attn: T. F. Ferger  
Post Office Box 1  
Mail Zone J-81  
Buffalo, New York 14205

Pratt & Whitney Aircraft  
Florida Research & Development  
Center  
Attn: G. D. Garrison  
Post Office Box 710  
West Palm Beach, Florida 33402

NASA  
Lewis Research Center  
Attn: L. Gordon, MS 500-209  
21000 Brookpark Road  
Cleveland Ohio 44135

Purdue University  
School of Mechanical Engineering  
Attn: R. Goulard  
Lafayette, Indiana 47907

Air Force Office of Scientific  
Research  
Chief Propulsion Division  
Attn: Lt. Col. R. W. Haffner (NAE)  
1400 Wilson Boulevard  
Arlington, Virginia 22209

University of Illinois  
Aeronautics/Astronautic Engineering  
Department  
Attn: R. A. Strehlow  
Transportation Building, Room 101  
Urbana, Illinois 61801

NASA  
Manned Spacecraft Center  
Attn: J. G. Thibadaux  
Houston, Texas 77058

Massachusetts Institute of Technology  
Department of Mechanical Engineering  
Attn: T. Y. Toong  
77 Massachusetts Avenue  
Cambridge, Massachusetts 02139

Illinois Institute of Technology  
Attn: T. P. Torda  
Room 200 MH.  
3300 S. Federal Street  
Chicago, Illinois 60616

AFRPL  
Attn: R. R. Weiss  
Edwards, California 93523

U. S. Army Missile Command  
AMSMI-RKL, Attn: W. W. Wharton  
Redstone Arsenal, Alabama 35808

University of California  
Aerospace Engineering Department  
Attn: F. A. Williams  
Post Office Box 109  
LaJolla, California 92037

Georgia Institute of Technology  
Aerospace School  
Attn: B. T. Zinn  
Atlanta, Georgia 30332

Marshall Industries  
Dynamic Science Division  
Attn: L. Zung  
2400 Michelson Drive  
Irvine, California 92664

Mr. Donald H. Dahlene  
U.S. Army Missile Command  
Research, Development, Engineering  
and Missile Systems Laboratory  
Attn: AMSMI-RK  
Redstone Arsenal, Alabama 35809

TISIA  
Defense Documentation Center  
Cameron Station  
Building 5  
5010 Duke Street  
Alexandria, Virginia 22314

Office of Assistant Director  
(Chemical Technician)  
Office of the Director of Defense  
Research and Engineering  
Washington, D. C. 20301

D. E. Mock  
Advanced Research Projects Agency  
Washington, D. C. 20525

Dr. H. K. Doetsch  
Arnold Engineering Development Center  
Air Force Systems Command  
Tullahoma, Tennessee 37389

Library  
Air Force Rocket Propulsion Laboratory  
(RPR)  
Edwards, California 93523

Library  
Bureau of Naval Weapons  
Department of the Navy  
Washington, D. C.

Library  
Director (Code 6180)  
U.S. Naval Research Laboratory  
Washington, D. C. 20390

APRP (Library)  
Air Force Aero Propulsion Laboratory  
Research and Technology Division  
Air Force Systems Command  
United States Air Force  
Wright-Patterson AFB, Ohio 45433

Technical Information Department  
Aeronutronic Division of Philco Ford  
Corporation  
Ford Road  
Newport Beach, California 92663

Library-Documents  
Aerospace Corporation  
2400 E. El Segundo Boulevard  
Los Angeles, California 90045

Princeton University  
James Forrestal Campus Library  
Attn: D. Harrje  
Post Office Box 710  
Princeton, New Jersey 08540

U.S. Naval Weapons Center  
Attn: T. Inouye, Code 4581  
China Lake, California 93555

Office of Naval Research  
Navy Department  
Attn: R. D. Jackel, 473  
Washington, D. C. 20360

Air Force Aero Propulsion Laboratory  
Attn: APTC Lt. M. Johnson  
Wright Patterson AFB, Ohio 45433

Naval Underwater Systems Center  
Energy Conversion Department  
Attn: Dr. R. S. Lazar, Code TB 131

NASA  
Langley Research Center  
Attn: R. S. Levine, MS 213  
Hampton, Virginia 23365

Aerojet General Corporation  
Attn: J. M. McBride  
Post Office Box 15847  
Sacramento, California 95809

Colorado State University  
Mechanical Engineering Department  
Attn: C. E. Mitchell  
Fort Collins, Colorado 80521

University of Wisconsin  
Mechanical Engineering Department  
Attn: P. S. Myers  
1513 University Avenue  
Madison, Wisconsin 53706

North American Rockwell Corporation  
Rocketdyne Division  
Attn: J. A. Nestlerode,  
AC46 D/596-121  
6633 Canoga Avenue  
Canoga Park, California 91304

University of Michigan  
Aerospace Engineering  
Attn: J. A. Nicholls  
Ann Arbor, Michigan 48104

Tulane University  
Attn: J. C. O'Harra  
6823 St. Charles Avenue  
New Orleans, Louisiana 70118

University of California  
Department of Chemical Engineering  
Attn: A. K. Oppenheim  
6161 Etcheverry Hall  
Berkeley, California 94720

Army Ballistics Laboratories  
Attn: J. R. Osborn  
Aberdeen Proving Ground, Maryland 21005

Sacramento State College  
School of Engineering  
Attn: F. H. Reardon  
6000 J. Street  
Sacramento, California 95819

Purdue University  
School of Mechanical Engineering  
Attn: B. A. Reese  
Lafayette, Indiana 47907

NASA  
George C. Marshall Space Flight Center  
Attn: R. J. Richmond, SNE-ASTN-PP  
Huntsville, Alabama 35812

Jet Propulsion Laboratory  
California Institute of Technology  
Attn: J. H. Rupe  
4800 Oak Grove Drive  
Pasadena, California 91103

University of California  
Mechanical Engineering Thermal Systems  
Attn: Prof. R. Sawyer  
Berkeley, California 94720

ARL (ARC)  
Attn: K. Scheller  
Wright Patterson AFB, Ohio 45433

Library  
Bell Aerosystems, Inc.  
Box 1  
Buffalo, New York 14205

Report Library, Room 6A  
Battelle Memorial Institute  
505 King Avenue  
Columbus, Ohio 43201

D. Suichu  
General Electric Company  
Flight Propulsion Laboratory Department  
Cincinnati, Ohio 45215

Library  
Ling-Temco-Vought Corporation  
Post Office Box 5907  
Dallas, Texas 75222

Marquardt Corporation  
16555 Saticoy Street  
Box 2013 - South Annex  
Van Nuys, California 91409

P. F. Winternitz  
New York University  
University Heights  
New York, New York

I. Forsten  
Picatinny Arsenal  
Dover, New Jersey 07801

R. Stiff  
Propulsion Division  
Aerojet-General Corporation  
Post Office Box 15847  
Sacramento, California 95803

Library, Department 596-306  
Rocketdyne Division of Rockwell  
North American Rockwell Inc.  
6633 Canoga Avenue  
Canoga Park California 91304

Library  
Stanford Research Institute  
333 Ravenswood Avenue  
Menlo Park, California 94025

Library  
Susquehanna Corporation  
Atlantic Research Division  
Shirley Highway and Edsall Road  
Alexandria, Virginia 22314

STL Tech. Lib. Doc. Acquisitions  
TRW System Group  
1 Space Park  
Redondo Beach, California 90278

Dr. David Altman  
United Aircraft Corporation  
United Technology Center  
Post Office Box 358  
Sunnyvale, California 94088

Library  
United Aircraft Corporation  
Pratt and Whitney Division  
Florida Research and Development  
Center  
Post Office Box 2691  
West Palm Beach, Florida 33402

Library  
Air Force Rocket Propulsion  
Laboratory (RPM)  
Edwards, California 93523

Allan Hribar, Assistant Professor  
Post Office Box 5014  
Tennessee Technological University  
Cookeville, Tennessee 38501

NASA Lewis Research Center  
Attn: E. O. Bourke MS 500-209  
21000 Brookpark Road  
Cleveland, Ohio 44135

NASA  
Lewis Research Center  
Attn: D. L. Nored 500-203  
21000 Brookpark Road  
Cleveland, Ohio 44135

NASA  
Lewis Research Center MS 500-313  
Rockets & Spacecraft Procurement Section  
21000 Brookpark Road  
Cleveland, Ohio 44135